

A model investigation of vegetation-atmosphere interactions on a millennial timescale

N Devaraju¹, Long Cao², G. Bala¹, Ken Caldeira², and Ramakrishna Nemani³

¹*Divecha Center for Climate Change and Center for Atmospheric and Oceanic Sciences, Indian Institute of Science, Bangalore – 560 012, India*

²*Department of Global Ecology, Carnegie Institution, 260 Panama Street, Stanford, CA 94305, USA*

³*NASA Ames Research Center, Moffett Field, CA 94035, USA*

Correspondence to: Devaraju N (dev@caos.iisc.ernet.in)

Abstract

A terrestrial biosphere model with dynamic vegetation capability, Integrated Biosphere Simulator (IBIS2), coupled to the NCAR Community Atmosphere Model (CAM2) is used to investigate the multiple climate-forest equilibrium states of the climate system. A 1000-year control simulation and another 1000-year land cover change simulation that consisted of global deforestation for 100 years followed by re-growth of forests for the subsequent 900 years were performed. After several centuries of interactive climate-vegetation dynamics, the land cover change simulation converged to essentially the same climate state as the control simulation. However, the climate system takes about a millennium to reach the control forest state. In the absence of deep ocean feedbacks in our model, the millennial time scale for converging to the original climate state is dictated by long time scales of the vegetation dynamics in the northern high latitudes. Our idealized modeling study suggests that the equilibrium state reached after complete global deforestation followed by re-growth of forests is unlikely to be distinguishable from the control climate. The real world, however, could have multiple climate-forest states since our modeling study is unlikely to have represented all the essential ecological processes (e.g. altered fire regimes, seed sources and seedling establishment dynamics) for the re-establishment of major biomes.

36 **1. Introduction**

37
38 Deforestation has both biogeochemical and biogeophysical influences on the climate: besides
39 releasing carbon from land to the atmosphere (a biogeochemical effect), deforestation also has
40 biogeophysical effects such as changes in land surface albedo, surface roughness, surface energy
41 fluxes, and cloud cover (Betts et al., 1996; Govindasamy et al., 2001; Betts 2001; Brovkin et al.,
42 1999; Feddema et al., 2005; Brovkin et al., 2006; Bala et al., 2007; Bonan, 2008; Brovkin et al.,
43 2009; Findell et al., 2009). Thus, land cover changes alter the climate through physical,
44 chemical, and biological processes and thereby could affect temperature, the hydrologic cycle,
45 and atmospheric composition.

46
47 Recently, Davin and Noblet-Ducoudre (2010) found that the biogeophysical (i.e. albedo change
48 and evapotranspiration) impact of global deforestation leads to global cooling of 1K because the
49 albedo effect is dominant over evapotranspiration. Lawrence and Chase (2010) and Xu et al.,
50 (2009) found that for land cover change, surface hydrology and its interaction with vegetation
51 and soils also has large impacts on the climate. Changes in land cover can also have remote
52 effects: Chen et al., (2001), Snyder et al., (2004) and Avissar et al., (2004) have found that
53 tropical deforestation is likely to induce changes in atmospheric circulation, and that these
54 changes may have consequences on precipitation and temperature patterns on a global scale.

55
56 In view of the aforementioned climate effects of land cover change there is a need to understand
57 the impact of large perturbations to land cover. Are there interactions between forests and the
58 atmosphere (i.e. vegetation-precipitation feedback, vegetation-temperature feedback) that gets
59 severely altered for large scale land cover change? Specifically, if deforested areas are
60 abandoned and forests are allowed to re-grow, will the climate system go back to its natural
61 state? How long will it take for the climate system to reach a new equilibrium in such a case?
62 What determines the time scale? We will address these questions in this paper using a dynamic
63 vegetation model coupled to an atmospheric general circulation model. Our model has
64 representation for dynamic vegetation, interaction between atmosphere and land surface via
65 temperature precipitation, soil moisture and plant water uptake but it lacks detailed
66 representation for nitrogen cycle, evolution of atmospheric CO₂, disturbance such as fires and
67 pests, anthropogenic land cover change, and management of forests. Therefore, our investigation

68 mainly aims to find out if interaction among atmosphere, land biophysics and dynamic natural
69 potential vegetation will result in multiple equilibriums.

70

71 Multiple steady states in the atmosphere biosphere system can arise as a consequence of positive
72 feedbacks between atmosphere and land surface. Claussen (1994, 1998) and Claussen et al.,
73 (1998) find that multiple vegetation–climate states can exist in the present-day semi-desert
74 regions of northern Africa and western Asia. A modeling study by Levis et al., (1999) and
75 Brovkin et al., (2003) find only one possible stable steady state in the climate system in the high
76 latitudes while bi-stable vegetation-climate states are found in models for the Amazon by Oyama
77 and Nobre (2003), and for Central-Asia and North-Africa by Claussen (1998). Wang and Eltahir
78 (2000) study the stability of similar states in response to disturbances. Brovkin et al., (1998) uses
79 a conceptual model to compare desert versus “green” equilibrium under parameter estimates
80 typical of current climate and of mid-Holocene climate, respectively.

81

82 Kleidon et al. (2007) find that multiple steady states occur in their earth system model of
83 intermediate complexity only if vegetation is represented by a few vegetation classes. With an
84 increased number of classes, the difference between the numbers of multiple steady states
85 diminishes and disappears completely when vegetation is represented by 8 classes or more in
86 their model. The two major positive vegetation feedbacks that result in the emergence of
87 multiple steady states are related to the temperature limitation on productivity in high latitudes
88 and the water limitation in the tropics and subtropics.

89

90 The possibility of multiple forest-climate states in the climate system has been investigated
91 recently by Brovkin et al., (2009) in the Earth System Model of the Max Planck Institute for
92 Meteorology (MPI-ESM). In their study, when the geographic distributions of vegetation in
93 forest-only and grassland-only simulations are allowed to interactively respond to climate, both
94 forest and grassland simulations converge to essentially the same climate state as in the control
95 simulation after subsequent 500 years of interactive climate-vegetation dynamics. This
96 convergence suggests an absence of multiple climate-forest states in MPI-ESM. Dekker et al.,
97 (2010), using an Earth Model of Intermediate Complexity, PlaSim, find that model integrations
98 starting from different initial biomass distributions diverge to clearly distinct climate-vegetation

99 states in terms of climatic (precipitation and temperature) and biotic (biomass) variables. Their
100 simulations suggest that the boreal and monsoon regions have low resilience, i.e. unstable
101 biomass equilibrium with positive vegetation-climate feedbacks in which the biomass change
102 induced by a perturbation is further enhanced. Large perturbations trigger an abrupt shift of the
103 system towards another steady state, and hence, Dekker et al., (2010) stress the importance of
104 coupling at multiple scales in vegetation-climate models and indicate the urgent need to
105 understand the system dynamics for improved projections of ecosystem responses to
106 anthropogenic changes in climate forcing.

107
108 In the present study, we investigate the possibility of multiple states in the climate system by
109 carrying out transient simulations using the NCAR atmospheric general circulation model CAM
110 (Community Atmosphere model) coupled to a dynamic vegetation model and a mixed layer
111 ocean model. Our objective is to use another model to simulate the vegetation dynamics to
112 understand whether, when and how positive climate-vegetation feedbacks will lead to multiple
113 steady states. We perform a millennial time scale simulation using a comprehensive coupled
114 atmospheric general circulation model and a terrestrial biosphere model to investigate the
115 possibility of multiple states. We show that the climate-vegetation system has no multiple steady
116 states in this modeling study but it takes nearly a millennium for the system to return to the initial
117 equilibrium state due to long time scales of vegetation dynamics in the northern high latitudes.
118 As a caveat, we note that our simulations are idealized and intended to understand the earth
119 system behavior for possible multiple climate-forest states. This study is not intended to
120 realistically represent current or future land cover change

121

122 **2. Model description**

123

124 The coupled climate-vegetation model used is Integrated Biosphere Simulator (IBIS2) (Foley et
125 al., 1996, Kucharik et al., 2000) coupled to Community Atmosphere Model 2.0 of NCAR
126 (CAM2) (Collins et al., 2004). We used the finite volume configuration of the model with a
127 horizontal resolution of 2° latitude and 2.5° longitude. There are 26 vertical levels. For this
128 study, we coupled CAM2 to a mixed layer ocean and thermodynamic sea ice model, which
129 allows for interactive surface for the ocean and sea ice components of the climate system.

130

131 Land surface biophysics, terrestrial carbon flux and global vegetation dynamics are represented
132 in a single, physically consistent modelling framework within IBIS2. IBIS2 simulates a variety
133 of ecosystem processes including energy, water, and carbon dioxide exchanges between soil,
134 plants and the atmosphere, physiological processes of plants (photosynthesis and respiration),
135 soil biogeochemistry, vegetation phenology including budburst, senescence, and dormancy of
136 vegetation, plant growth and competition, nutrient cycling and soil physics. The coupled
137 simulation of surface water, energy and carbon fluxes are performed on hourly time steps and
138 integrated over the year to estimate annual water and carbon balance. The annual carbon balance
139 of vegetation is used to predict changes in the leaf area index and biomass for each of 12 plant
140 functional types, which compete for light and water using different ecological strategies. IBIS2
141 also simulates carbon cycling through litter and soil organic matter. When driven by observed
142 climatological datasets, the model's near-equilibrium runoff, net primary productivity (NPP),
143 and vegetation categories show a fair degree of agreement with observations (Foley et al., 1996,
144 Kucharik et al., 2000).

145 146 **3. Experiments**

147
148 We first performed a long simulation with prescribed climatological sea surface temperatures
149 (SST) and a round number of present day CO₂ concentration of 400 ppm to calculate the implied
150 ocean heat transport which is needed to use CAM2 in slab ocean configuration. For this
151 climatological-SST simulation, we used a soil carbon spin up factor of 40 and ran the model until
152 biomass and soil carbon reached quasi equilibrium. A soil carbon drift of less than 0.1 Gt-C per
153 year is used to define the quasi equilibrium state. The implied ocean heat transport is calculated
154 after soil carbon reached equilibrium. Then, we used this spun-up state of the biosphere model in
155 a 200 year mixed layer simulation until the soil carbon again reached quasi equilibrium. From
156 this state, we performed two 1000-year mixed layer simulations as described below.

157
158 1) a control simulation corresponding to present day conditions , 2) a land cover change
159 simulation, denoted by "LCC", where we do not allow tree plant functional types (PFTs) to exist
160 globally for 100 years; only grasses and shrubs are allowed. The biomass in tree leaves and fine
161 roots is immediately (year 1) transferred to the litter pool, and the stem biomass becomes litter
162 on a time scale of 10–50 years depending on the tree plant functional type. After 100 years, all

163 PFTs are allowed to exist for the subsequent 900 years. By 100 years, majority of the biomass
164 would be transferred to the litter pool and hence we choose this time scale for the deforested
165 period. We choose 900 years for the re-growth period because that is the time it took for the
166 coupled vegetation- climate system in this model to reach a quasi equilibrium state. The climate
167 statistics presented below are the averaged values over the last 100 years of model simulations.
168 The statistical significance here is tested using the student t-test with correction for lag-1
169 autocorrelation (Zwiers and von Storch, 1995).

170

171 Since our model is not a comprehensive earth system model with deep-ocean and ocean carbon
172 cycle, we do not have the formulation for tracking the carbon and accounting for the carbon
173 budget in this study. We have prescribed atmospheric CO₂ at a constant level (400 ppm)
174 throughout the simulation period and hence it serves as an infinite reservoir for carbon for the
175 terrestrial biosphere. In effect, we account for feedbacks due to biophysical effect of land cover
176 change (e.g. albedo, evapotranspiration, roughness length changes) but omit the biogeochemical
177 change since atmospheric CO₂ does not vary in response to land cover change.

178

179 **4. Results**

180

181 The temporal evolution of annual land mean key climate and terrestrial carbon cycle variables is
182 shown in Figure 1. In response to the instantaneous deforestation in LCC simulation, the land
183 surface temperature decreases by 3 K (1.7K over globe) averaged over the first 100 years and
184 land mean precipitation decreases by 14.4% (3.7 % over globe). The sign of the changes are
185 suggestive of the dominance of albedo effect (deforestation increases the surface reflectivity)
186 over changes in evapotranspiration and the associated cloud effects in this model. Global mean
187 temperature change (cooling) simulated in our study is comparable to another global land cover
188 change study that included only biogeophysical effect (1.3K in Gibbard et al., 2005) but higher
189 than obtained in Bala et al., (2007) because this later study also included the warming effect of
190 increased atmospheric CO₂ from deforestation (the carbon cycle effect).

191

192 When tree-PFTS are allowed from the deforested state, temperature and precipitation and other
193 variables show a fast recovery for about 100 years (Fig. 1) followed by a slow recovery for the
194 subsequent centuries . After 700 years of model integration with interactive climate-vegetation

195 dynamics from the deforested state, the land mean annual surface temperature and precipitation
196 in the LCC simulation slowly converges to essentially the same climate state (Fig. 1a-b) as that
197 of control simulation. Global mean surface temperature in LCC, averaged over the last century,
198 is higher than the control state by only 0.08°C. Since the standard deviation in the control is of
199 the same magnitude (0.07° C in control and 0.09° C in LCC), we conclude that the climate of the
200 last hundred years of LCC are indistinguishable from the control.

201
202 However, the time series of carbon cycle variables specifically the carbon stocks (Fig. 1c-d),
203 suggest that the terrestrial biosphere is still converging towards the new equilibrium state.
204 Immediately following deforestation, Net Primary Productivity (NPP) declines by 22% from 79
205 to 62 Gt-C per year since grasslands have, on an average, less NPP than forests in this model
206 (Fig. 1e). The “step-like” behavior of NPP at year 100 is due to “step-like” increase in gross
207 primary productivity since tree PFTs have higher LAI than grasses and shrubs. We used an
208 exponential fit (Eqn. 1, given below) and find that time scale of this rapid evolution is only about
209 2 years. There is also a slow recovery component which has a time scale of about 600 years.
210 There is no succession dynamics in the model and NPP is mainly dependent on the biomass in
211 leaves which has a time scale of 2 years in our model. We find that the time scale of slow
212 component is dictated by the recovery of NPP in high latitudes which is similar to the vegetation
213 fraction dynamics there as discussed below (Fig.2).

214
215 Net Ecosystem Exchange (NEE) represents the net land carbon uptake and is defined as NPP
216 minus soil respiration which includes both microbial decomposition and root respiration. It
217 shows declines and increases of similar magnitude to NPP after instantaneous deforestation and
218 immediately following re-growth of forests (Fig. 1f). The sharp decline of NEE by 18 Gt-C
219 immediately after deforestation is mainly due to the sharp decline in NPP. The subsequent
220 increase in NEE is mainly due to decrease in soil respiration (Fig. 1g). Re-growth of forests at
221 year 100 leads to a jump in NEE because of the step-function-like increase in NPP.
222 Subsequently, increase in soil respiration leads to the decline in NEE to control simulation levels.
223 The time scale of NEE recovery is about 100 years which is primarily dictated by the
224 decomposition time scale of dead stem biomass in the litter pool (Fig. 1h).

225

226 After deforestation, there is a large decline of about 800 Gt-C in biomass (Fig. 1c). Soil carbon
 227 increases(Fig.1d) by only about 120 Gt-C during this period because most of the dead biomass is
 228 transferred to the litter pool which transfers only a fraction to soil carbon pool and the rest
 229 decomposes from the litter pool. When forests are allowed to re-grow, there is a rapid recovery
 230 in biomass; it increases from less than 100 Gt-C to more than 800 Gt-C within 100 years. After
 231 this period, it asymptotically reaches the control simulation after several centuries. Soil carbon
 232 stock also shows a rapid recovery but it has about 20 Gt-C more than control even after 900
 233 years of re-growth. It should be noted that there is no conservation of total carbon stock (biomass
 234 plus soil carbon) in this study because atmospheric CO₂ is prescribed, providing an infinite
 235 reservoir for carbon to the terrestrial biosphere.

236
 237 The differences in annual precipitation values over land between the two runs at year 100 after
 238 trees allow growing are low (0.3 mm/day, Fig.1b). However the differences in biomass are large
 239 (Fig 1c). This implies that the moisture recycling due to vegetation changes is very low in this
 240 model setup. We also find similar evolution for tropical region which implies relatively small
 241 differences for the tropical regions in moisture recycling between control and LCC. Therefore,
 242 our model simulates low moisture recycling to vegetation changes and hence has low sensitivity
 243 to precipitation-vegetation feedbacks. This may be one of the causes for not simulating multiple
 244 climate-forest states in the model.

245
 246 The time evolution of global and regional tree cover area fraction is shown in Figure.2 We have
 247 fitted the tree cover fraction of LCC to an exponential form:

248
$$f = A_0 + A_1 \exp(-t / t_1) + A_2 \exp(-t / t_2) \dots\dots\dots (1)$$

249 where f is the fractional area of tree cover; A_0, A_1, A_2 are constants, t is time in years; and t_1 and
 250 t_2 are time scales in years. This exponential fit is applied to tree cover evolution simulated for
 251 global, tropical, mid latitude and high latitude regions. Table 1 lists the time scales thus obtained.
 252 When tree cover is allowed to recover, we see that the dynamics of tree cover converges faster in
 253 tropics (~ 4.5years). In mid latitudes, the dynamics is dominated by a 12 year fast time scale. In
 254 the high latitudes, a long time scale of 553 years dictates the evolution of tree cover suggesting

255 that the long time scale in the global tree cover comes from the dynamics of boreal tree cover
256 evolution.

257

258 To investigate the dynamics in the boreal region further, we plot the key climate and carbon
259 cycle variables for the latitudinal belt 50°N to 90°N in Fig. 3. The evolution of all the variables
260 are similar to the global-mean (Fig.1) but the time scales are much longer. As found in other
261 studies (Kleidon et al. 2007, Bala et al. 2006, Bonan 2008), it is likely that the feedback between
262 temperature (snow cover related albedo) and vegetation (tree cover extent) is primarily the cause
263 for the longer time scales that is simulated for the high latitudes (Fig. 3)

264

265 The spatial pattern of temperature change in LCC relative to control averaged over the last 100
266 years shows that the significant changes are seen in high latitudes (Fig. 4). Over the globe,
267 temperature changes over 11.8% (12.0 % over land) during the winter (DJF) and 13.8% (18.8%
268 over land) in the summer (JJA) are statistically significant at 5% level. The LCC simulation
269 produces in general more precipitation over land than the control simulation during both the DJF
270 and JJA seasons (Fig. 4c, d), and there is a reduction in the tropics. Precipitation changes over
271 globe are significant at the 5% level over 5.6% (8.3% over land) and 7.59% (9.4% over land) in
272 DJF and JJA seasons, respectively. In summary, Fig. 4 shows that spatial pattern of the physical
273 (abiotic) climate system in LCC is almost indistinguishable from the control.

274

275 Fig. 5 shows NPP, biomass and soil carbon in the LCC and control simulations and their
276 difference averaged over the last 100 years. In the control and LCC simulations, NPP and
277 biomass are larger in thickly vegetated regions of the world such as Amazon, central Africa,
278 South and Southeast Asia, Europe and eastern North America. There is a large bias in simulated
279 NPP and biomass in Australia when compared to a standard suite of global products
280 characterizing the NPP based on satellite observations (Fig. 5 in Running et al., 2004). Soil
281 carbon is also higher in places where NPP and biomass have larger values. In addition, soil
282 carbon has maxima in colder places such as Siberia, Alaska and the Himalayas. The spatial
283 pattern of NPP, biomass and soil carbon is similar in both control and LCC simulations.
284 Differences in these variables are small and mostly not significant except soil carbon differences
285 in some high latitude locations in Siberia and Alaska: the differences in NPP, biomass and soil

286 carbon are significant over 3.9, 21.3, and 25.2% of the land regions. Since the magnitudes of the
287 differences are small, we conclude that the spatial distribution of the terrestrial carbon fluxes and
288 carbon stocks (biotic component) in LCC in the last 100 years are also almost indistinguishable
289 from control.

290

291 The areal extent (in percentage) of simulated dominant vegetation types in the last 100 years in
292 LCC and control cases are given in Table 2. We found that the model simulates the locations of
293 major biomes reasonably well; tropical evergreen and deciduous forests in the tropics, temperate
294 forests in the mid latitudes and boreal forests in the high latitudes. However, there were major
295 biases such as the simulation of tropical and temperate forests in desert regions such as Saudi
296 Arabia, Australia and northern Africa and, consequently, an underestimation of deserts, Tundra
297 and polar desert regions. We identified that a warm and wet bias in the control simulation was
298 the main cause for these biases: the global and annual mean surface air temperature and
299 precipitation in the control simulation are higher by 1.3°C and 10% when compared to NCEP
300 reanalysis (Kistler et al., 2001) and GPCP (Adler et al., 2003), respectively.

301

302 We use kappa statistics (Monserud 1992) to compare vegetation distributions in LCC and
303 control. Kappa takes on a value of 1 with perfect agreement. It has a value close to zero when the
304 agreement is approximately the same as would be expected by chance. Global comparison of
305 vegetation distributions of LCC and control gives a kappa value of 0.93 (excellent agreement).
306 Except for Tundra, Kappa for major biomes between LCC and control suggests either excellent
307 or very good agreement (Table 2). The low value of Kappa for Tundra is partly related to the
308 smallest area occupied by Tundra in the control experiment (changes are relatively bigger for
309 Tundra) and partly because the vegetation dynamics has not yet reached equilibrium in the high
310 latitudes (Fig. 2d). This Kappa statistics suggests that the spatial distribution of the vegetation
311 state in LCC in the last 100 years is also almost indistinguishable from control.

312

313 **5. Discussion**

314

315 In this study, we examined the possibility of multiple climate-forest states using a terrestrial
316 biosphere model IBIS2 coupled to NCAR CAM2. For this purpose, we performed a global

317 deforestation experiment for 100 years followed by re-growth of forests. We find that there are
318 no multiple climate-forest states in our model; the simulation with deforestation followed by re-
319 growth converges to the control climate. Our conclusion is similar to a recent modeling study
320 (Brovkin et al., 2009) which also found an absence of multiple climate-forest states in the Earth
321 System Model of the Max Planck Institute for Meteorology, but different from another study by
322 Dekker et al., 2010 which found multiple equilibrium states. In our study, we find that the
323 climate system takes about 700 years to come back to the original natural state. This is despite
324 the fact that our simulation did not have representation for deep ocean feedbacks; we have used
325 only a mixed layer ocean model for representing the interaction between the atmosphere and
326 oceans. The millennial time scale for recovery in our model is dictated by the vegetation
327 dynamics in the high latitudes.

328
329 Brovkin et al 2009 uses a tiled structure of the land surface with 8 PFT's and two types of bare
330 surface but no biogeochemical effects of vegetation cover changes are included in their model
331 (JSBACH). Trees and grasses compete for free available area. IBIS2 uses 12 PFTs with grass
332 layer underneath the tree canopy. The biogeochemical effects of vegetation cover changes are
333 included. IBIS2 also has representation for soil biogeochemistry. Both models have differing
334 representation for competition among PFTs. Whether vegetation dynamics has multiple states or
335 not is apparently independent on these minor differences in the formulations between IBIS2 and
336 JSBACH. However, multiple vegetation states be may be inherent to vegetation models with
337 different formulations that are probably not be represented in IBIS2 and JSBACH (Dekker et al.
338 2010).

339
340 The dynamic vegetation model used in this study has some limitations: IBIS2 does not have
341 representation for nitrogen and other nutrient cycles (Cramer et al., 2001, McGuire et al., 2001,
342 Bala et al., 2007). IBIS2 model, in its current form, does not include a dynamic fire module
343 (Foley et al., 1996). It does not account for changes in pest attack or grazing by animal in a
344 changed climate. Suitable climatic conditions are sufficient for the existence of plant functional
345 types in IBIS2: seed dispersal mechanisms which are crucial for reestablishment of forests are
346 not represented. The real world, therefore, could have multiple climate-forest states, and this
347 present modeling study is unlikely to have represented all the essential ecological processes

348 (such as altered fire regimes, seed sources and seedling establishment dynamics) for the re-
349 establishment of major biomes.

350

351 The atmospheric conditions affect vegetation productivity in terms of available light, water and
352 heat, and different levels of vegetation productivity can result in differing energy and water
353 partitioning at the land surface, thereby leading to different atmospheric conditions. Kleidon et
354 al., 2007 find that if there are less number of discrete PFTs the climate conditions do not overlap
355 and multiple vegetation equilibria can result. With an increased number of classes the difference
356 between the numbers of multiple steady states diminishes and disappears completely when
357 vegetation is represented by 8 classes or more in their model. Therefore, it is possible that our
358 model with 12 PFTs has no multiple steady states. An analysis of the sensitivity of multiple
359 equilibriums to the number of PFTs and other parameters in the model is beyond the scope of
360 this paper and our future studies will investigate this.

361

362 Major limitations of this modelling study are the lack of deep-ocean dynamics, dynamic sea ice,
363 and representation of biogeochemical effects of vegetation cover changes and ocean carbon
364 cycle. As discussed before, the effect of changes in atmospheric CO₂ from deforestation and
365 interactive vegetation is not modeled in this study. For instance, we have overestimated the
366 amount of cooling immediately after deforestation on shorter time scales because we have not
367 included the effect of CO₂ emission from deforestation. However, on centennial to millennial
368 time scale the ocean biogeochemistry could buffer most of the atmospheric CO₂ changes induced
369 by an altered land cover. Future modelling on the investigation of multiple climate-forest states
370 should use coupled climate and carbon cycle models that will have realistic representation of
371 these long term feedbacks in the climate system.

372

373 The results discussed in this paper are from a single modelling study. Climate model differ in
374 their representation of physical processes and hence models show differing sensitivities to
375 climate perturbations. Many of the local and remote effects depend heavily on the model
376 structure and the simulated effects are therefore subject to have a wide range. Therefore, an
377 intercomparison of multiple models in the future will be required to investigate robustness in the
378 behaviour climate system.

379 **Acknowledgement**

380 Financial support for Dr. Devaraju was provided by the Divecha Center for Climate Change, Indian
381 Institute of Science. Suggestions and comments by the two anonymous reviewers helped us to improve
382 the manuscript substantially.

383

384 **References:**

385
386
387
388
389
390
391
392
393
394
395
396
397
398
399
400
401
402
403
404
405
406
407
408
409
410
411
412
413
414
415
416
417
418
419
420
421
422
423
424
425
426
427
428

1. Adler, R. F., Huffman, G. J., Chang, A., Ferraro, R., Xie, P.-P., Janowiak, J., Rudolf, B., Schneider, U., Curtis, S., Bolvin, D., Gruber, A., Susskind, J., Arkin, P., and Nelkin, E.: The version-2 Global Precipitation Climatology Project (GPCP) monthly precipitation analysis (1979-present), *J. Hydrometeor.* 4 ,1147-1167, 2003.
2. Avissar, R., R.R. da Silva, and D. Werth: Implications of tropical deforestation for regional and global hydroclimate, *Ecosystems and Land Use Change* 153, 73-83, 2004.
3. Bala, G., K. Caldeira, M. Wickett, T. J. Phillips, D. B. Lobell, C. Delire, and A. Mirin : Combined climate and carbon-cycle effects of large-scale deforestation. *Proc. Natl. Acad. Sci. U.S.A.* 104(16), 6550-6555, 2007.
4. Bala, G., Caldeira, K. , Mirin, A., Wickett, M., and Delire, C.: Direct effects of CO₂-fertilization on climate, *Tellus* 58B, 620-627, 2006.
5. Betts A.K, J.H. Ball, A.C.M. Beljaars, M.J. Miller and P.A. Viterbo: The land surface-atmosphere interaction: A review based on observational and global modeling perspectives, *J. Geo. Res.* 101(D3), 7209-7225, 1996.
6. Betts, R. A.: Biogeophysical impacts of land use on present-day climate: Near-surface temperature change and radiative forcing, *Atmos. Sci. Lett.*, 2, 39–51, 2001.
7. Bonan, G. : Forests and climate change: forcings, feedbacks and the climate benefits of forests, *Science*, 320, 1444-1449, 2008.
8. Brovkin, V., Claussen, M., Driesschaert, E., Fichefet, T., Kicklighter, D., Loutre, M. F., Matthews, H. D., Ramankutty, N., Schaeffer, M., and Sokolov, A.: Biogeophysical effects of historical land cover changes simulated by six Earth system models of intermediate complexity, *Climate Dyn.*, 26, 587–600, 2006.
9. Brovkin, V., A. Ganopolski, M. Claussen, C. Kubatzki, and V. Petoukhov: Modelling climate response to historical land cover change, *Global Ecol. Biogeogr.*, 8, 509–517, 1999.
10. Brovkin, V., M. Claussen, V. Petoukhov, and A. Ganopolski: On the stability of the atmosphere–vegetation system in the Sahara Sahel region, *J. Geophys. Res.*, 103, 31613–31624, 1998.
11. Brovkin, V., Levis, S., Loutre, M.-F., Crucifix, M., Claussen, M., Ganopolski, A., Kubatzki, C., and Petoukhov, V.: Stability analysis of the climate-vegetation system in the northern high latitudes, *Climate. Change*, 57, 119–138, 2003.

- 429 12. Brovkin, V., Raddatz, T., Reick, C. H., Claussen, M., and Gayler, V.: Global
430 biogeophysical interactions between forest and climate, *Geophys. Res. Lett.*, 36, L07405,
431 doi:10.1029/2009GL037543, 2009.
432
- 433 13. Chen, T.C., J.H. Yoon, K.J. St. Croix, and E.S. Takle : Suppressing impacts of the
434 Amazonian deforestation by the global circulation change, *Bull. Am. Met. Soc.*, 82, 2209-
435 2216, 2001.
436
- 437 14. Claussen, M.: On coupling global biome models with climate models, *Climate Res.*, 4 ,
438 203–221, 1994.
439
- 440 15. Claussen, M.: On multiple solutions of the atmosphere–vegetation system in present-day
441 climate, *Global Biogeochem. Cycles*, 4, 549–559, 1998.
442
- 443 16. Claussen, M., Brovkin, V., Ganopolski, A. and Kubatzki, C.: Modelling global terrestrial
444 vegetation–climate interaction, *Philos. Trans. Roy. Soc. London*, 353B, 53–63, 1998.
445
- 446 17. Collins, W., Blackmon, D. M., Bitz, C., Bonan, G., Bretherton, C. S., Carton, J. A.,
447 Chang, P., Doney, S., Hack, J. J., Kiel, J. T., Henderson, T., Large, W. G., McKenna, D.,
448 Santer, B. D., and Smith, R. D.: Description of the NCAR community atmosphere model
449 (CAM 3. 0), Tech. Note NCAR/TN–464+STR, Natl. Cent. Atmos. Res., Boulder,
450 Colorado, 2004.
451
- 452 18. Cramer, W., Bondeau, A., Woodward, F. I., Prentice, I. C., Betts, R. A., Brovkin, V.,
453 Cox, P. M., Fisher, V., Foley, J. A., Friend, A. D., Kucharik, C., Lomas, M. R.,
454 Ramankutty, N., Sitch, S., Smith, B., White, A., Young-Molling, C.: Global response of
455 terrestrial ecosystem structure and function to CO₂ and climate change: Results from six
456 dynamic global vegetation models, *Global Change Biol.*, 7, 357 – 373, 2001.
457
- 458 19. Davin, E.L. and N. Noblet-Ducoudre: Climatic impact of global-scale deforestation:
459 radiative versus nonradiative processes, *J. Climate*, 23, 97-112, 2010.
460
- 461 20. Dekker, S. C., H. J. de Boer, V. Brovkin, K. Fraedrich, M. J. Wassen, and M. Rietkerk :
462 Biogeophysical feedbacks trigger shifts in the modeled vegetation-atmosphere system at
463 multiple scales, *Biogeosciences*, 7, 1237–1245, 2010.
464
- 465 21. Feddema, J., K. Oleson, G. Bonan, L. Mearns, W. Washington, G. Meehl, and D. Nychka
466 : A comparison of a GCM response to historical anthropogenic land cover change and
467 model sensitivity to uncertainty in present-day land cover representations, *Climate Dyn.*,
468 25, 581–609, 2005.
469
- 470 22. Findell, K. L., A.J. Pitman, Mathew, H.E. and P. J. Pegion: Regional and global impacts
471 of land cover change and sea surface temperature anomalies, *J. Clim.*, 22, 3248–3269,
472 2009.
473

- 474 23. Foley, J. A., I. C. Prentice, N. Ramankutty, S. Levis, D. Pollard, S. Sitch, and A.
475 Haxeltine: An integrated biosphere model of land surface processes, terrestrial carbon
476 balance and vegetation dynamics, *Global Biogeochem. Cycles*, 10, 603– 628, 1996.
477
- 478 24. Gibbard, S. G., K. Caldeira, G. Bala, T.J. Phillips and M. Wickett : Climate effects of
479 global land cover change, *Geophys. Res. Lett.*, 32, L23705, doi:10.1029/2005GL024550,
480 2005.
481
- 482 25. Govindasamy, B., P. B. Duffy, and K. Caldeira, Land use changes and Northern
483 Hemisphere cooling, *Geophys. Res. Lett.*, 28, 291–294, 2001.
484
- 485 26. Kistler, R., Kalnay, E., Collins, W., Saha, S., White, G., Woollen, J., Chelliah, M.,
486 Ebisuzaki, W., Kanamitsu, M., Kousky, V., van den Dool, H., Jenne, R., and Fiorino, M.:
487 The NCEP-NCAR 50 –year reanalysis: Monthly means CD-ROM and documentation,
488 *Bull. Amer. Meteor. Soc.*, 82, 247-267, 2001.
489
- 490 27. Kleidon, A., K. Fraedrich, and C. Low: Multiple steady states in the terrestrial
491 atmosphere-biosphere system: a result of a discrete vegetation classification?
492 *Biogeosciences*, 4, 707-714, 2007.
493
- 494 28. Kucharik, C. J., Foley, J. A., Delire, C., Fisher, V. A., Coe, M. T., Lenters, J. D., Young-
495 Molling, C., Ramankutty, N., Norman, J. M., and Gower, T.: Testing the performance of a
496 dynamic global ecosystem model: Water balance, carbon balance, and vegetation
497 structure, *Global Biogeochem. Cycles*, 14(3), 795, 2000.
498
- 499 29. Lawrence P.J., Thomas, N., and Chase, T.N.: Investigating the climate impacts of global
500 land cover change in the community climate system model, *Int. J. Climatol.*, 30(13), 2066-
501 2087, 2010. (DOI: 10.1002/joc.2061)
502
- 503 30. Levis, S., J.A. Foley, V. Brovkin, D. Pollard : On the stability of the high latitude climate-
504 vegetation system in a coupled atmosphere-biosphere model, *Glob. Ecol. Biogeogr.*, 8,
505 489-500, 1999.
506
- 507 31. McGuire, A. D., Sitch, S., Clein, J. S., Dargaville, R., Esser, G., Foley, J., Heimann, M.,
508 Joos, F., Kaplan, J., Kicklighter, D. W., Meier, R. A., Melillo, J. M., Moore, B., Prentice,
509 I. C., Ramankutty, N., Reichenau, T., Schloss, A., Tian, H., Williams, L. J., and
510 Wittenberg, U.: Carbon balance of the terrestrial biosphere in the twentieth century:
511 analyses of CO₂, climate and land use effects with four process-based ecosystem models,
512 *Global Biogeochemical Cycles*, 15, 183–206, 2001.
513
- 514 32. Monserud, R.A. and Leemans, R. : Comparing global vegetation maps with the Kappa
515 statistic, *Ecol. Model.*, 62, 275-293, 1992.
516
- 517 33. Oyama, M. D. and Nobre, C. A.: A new climate-vegetation equilibrium state for tropical
518 South America, *Geophys. Res. Lett.*, 30(4) 2199, 2003.
519

520 34. Running, S.W., R.R. Nemani, F.A. Heinsch, M. Zhao, M. Reeves and H. Hashimoto: A
521 continuous satellite-derived measure of global terrestrial production, *BioScience*, 54,
522 547–560, 2004.
523

524 35. Snyder, P.K., J.A. Foley, M.H. Hitchman, and C. Delire: Analyzing the effects of
525 complete tropical forest removal on the regional climate using a detailed three
526 dimensional energy budget: An application to Africa, *J. Geophys. Res. Atmospheres*, 109
527 (D21102), doi:10.1029/2003JD004462, 2004.
528

529 36. Wang, G., and E. A. B. Eltahir: Biosphere–atmosphere interactions over West Africa. 2.
530 Multiple climate equilibria, *Quart. J. Roy. Meteor. Soc.*, 126(565) 1261-1280, 2000.
531

532 37. Zhongfeng, X., Gang, Z., and Congbin, F.: Global and Regional Impacts of Vegetation
533 on the Hydrological Cycle and Energy Budget as Represented by the Community
534 Atmosphere Model (CAM3), *Atm. and Oceanic Sci. Lett.*, 2(2), 85–90, 2009.
535

536 38. Zwiers, F. W. 5 and von Storch, H.: Taking serial correlation into account in tests of the
537 mean, *J. Climate*, 8, 336-351, 1995.
538
539
540
541
542
543
544
545
546
547
548
549
550
551
552
553
554
555
556
557
558
559
560
561
562
563

564 **Table 1. Values of the constants in the exponential fit (Eqn. 1) for the dynamics of**
 565 **fractional tree cover (f) plotted in Fig.2 for different regions (Globe, Boreal (50⁰N-90⁰N),**
 566 **mid latitudes (20⁰N-50⁰N) and Tropics (20⁰S-20⁰N)) in the LCC simulation**
 567

Tree Cover Dynamics ⇒	$f = A_0 + A_1 \exp(-t/t_1) + A_2 \exp(-t/t_2)$ 568 (applied to 101-1000 years of the LCC simulation) 569				
	t ₁ (years)	t ₂ (years)	A ₀	A ₁	A ₂ 570
Regions ↓					
Globe	7.3	274	0.68	-0.64	-0.08 571
Tropics	4.5	--	0.91	-0.68	0 572
Northern Mid Latitudes	12	171	0.55	-0.46	-0.07 573
Northern High Latitudes	22	553	0.77	-0.20	-0.27 574

582
 583
 584
 585

586
587
588

Table 2. Areal extent of dominant vegetation types and Kappa statistics

Dominant Vegetation type	Control (%)	LCC (%)	Kappa Statistics	Degree of Agreement
Tropical Evergreen	22.8	22.9	0.96	Excellent
Tropical deciduous	13.8	13.8	0.93	Excellent
Temperate	20.9	20.5	0.95	Excellent
Boreal	12.0	12.1	0.85	Excellent
Savana, Grasslands and Shrublands	15.0	14.1	0.83	Very good
Tundra	3.2	3.9	0.39	Poor
Desert	4.8	5.0	0.95	Excellent
Ice	7.5	7.7	0.81	Very good
Global Vegetation	100	100	0.93	Excellent

589
590
591

592 **Figure Captions**

593

594 **Figure 1.** Evolution of annual mean a) land surface temperature, b) precipitation over land, c)
595 biomass, d) soil carbon, e) net primary productivity (NPP), f) net ecosystem exchange (NEE), g)
596 soil respiration (includes heterotrophic respiration and disturbances) , and h) total litter for the
597 1000-yr control and LCC simulations.

598

599 **Figure 2.** Evolution of global, tropical (20°S to 20°N), mid latitude (20°N to 50°N), and high
600 latitude (50° N to 90°N) annual mean fractional area of tree cover in the LCC simulation
601 (Tropical evergreen, Tropical deciduous, Temperate and Boreal forests).

602

603 **Figure 3.** Evolution of annual mean a) land surface temperature, b) precipitation over land, c)
604 biomass, d) soil carbon, e) net primary productivity (NPP), f) net ecosystem exchange (NEE), g)
605 soil respiration (includes heterotrophic respiration and disturbances) , and h) total litter for the
606 1000-yr control and LCC simulations in the northern hemisphere high latitudes(50°N – 90° N).

607

608 **Figure 4.** Mean differences between LCC and control simulations for surface Temperature (°C)
609 in (a) winter (DJF), (b) summer (JJA) , and precipitation (mm/day) in (c) winter (DJF), and (d)
610 summer (JJA). Mean differences are obtained by averaging over the last 100 years. Hatched
611 areas are regions where changes are statistically significant at the 95% confidence level.
612 Significance level is estimated using a Student-t test with a sample of 100 annual means and
613 standard error corrected for temporal autocorrelation (Zwiers and von Storch ,1995)

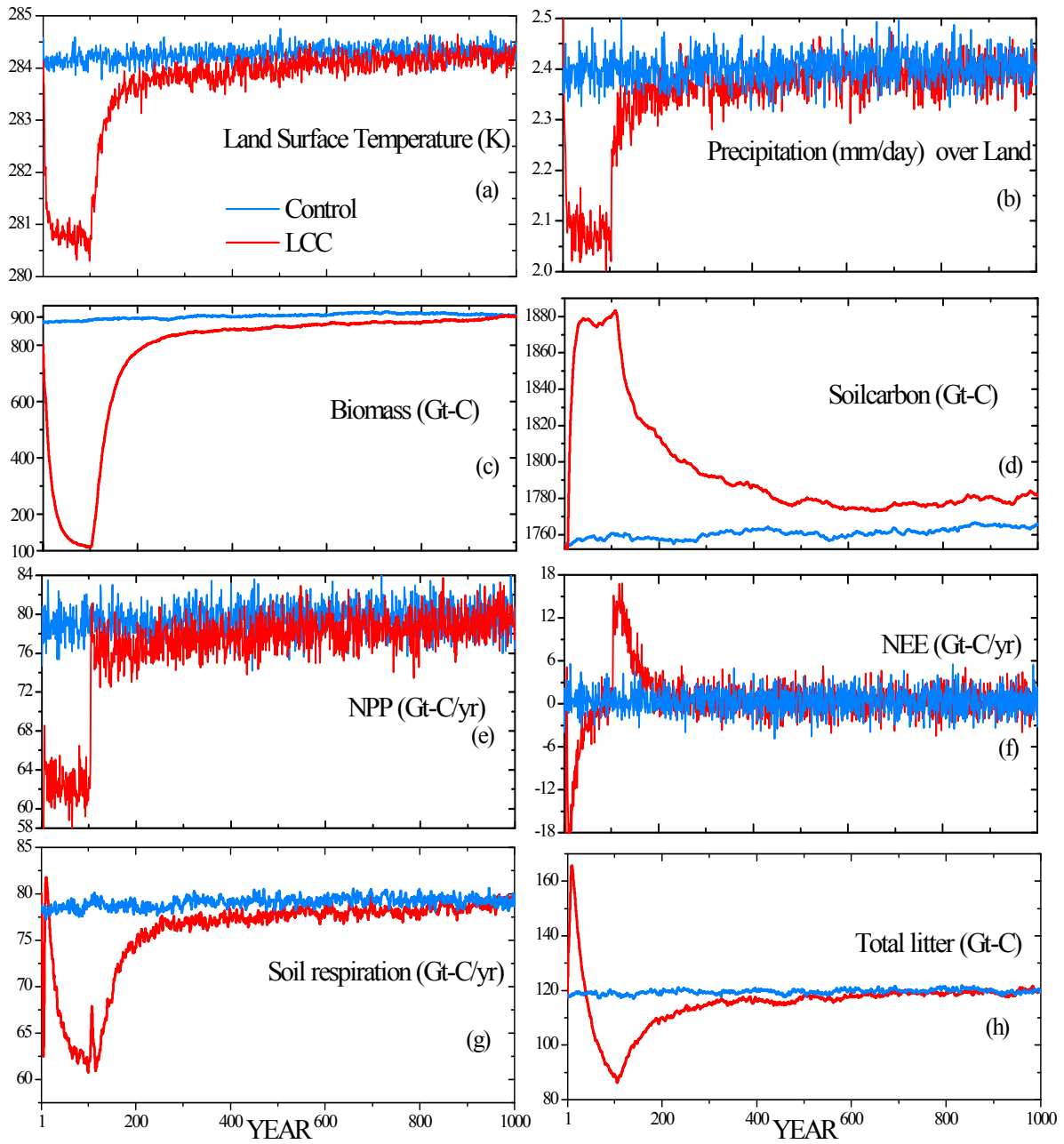
614

615 **Figure 5.** Comparison between LCC and control simulations for terrestrial biosphere variables.
616 The first and second column panels represent 100-year mean from the control and LCC
617 simulations, respectively. The third column panels represent the difference between LCC and the
618 control simulations. Hatched areas are regions where changes are statistically significant at the
619 95% confidence level. Significance level is estimated using a Student-t test with a sample of 100
620 means and standard error corrected for autocorrelation (Zwiers and von Storch, 1995)

621

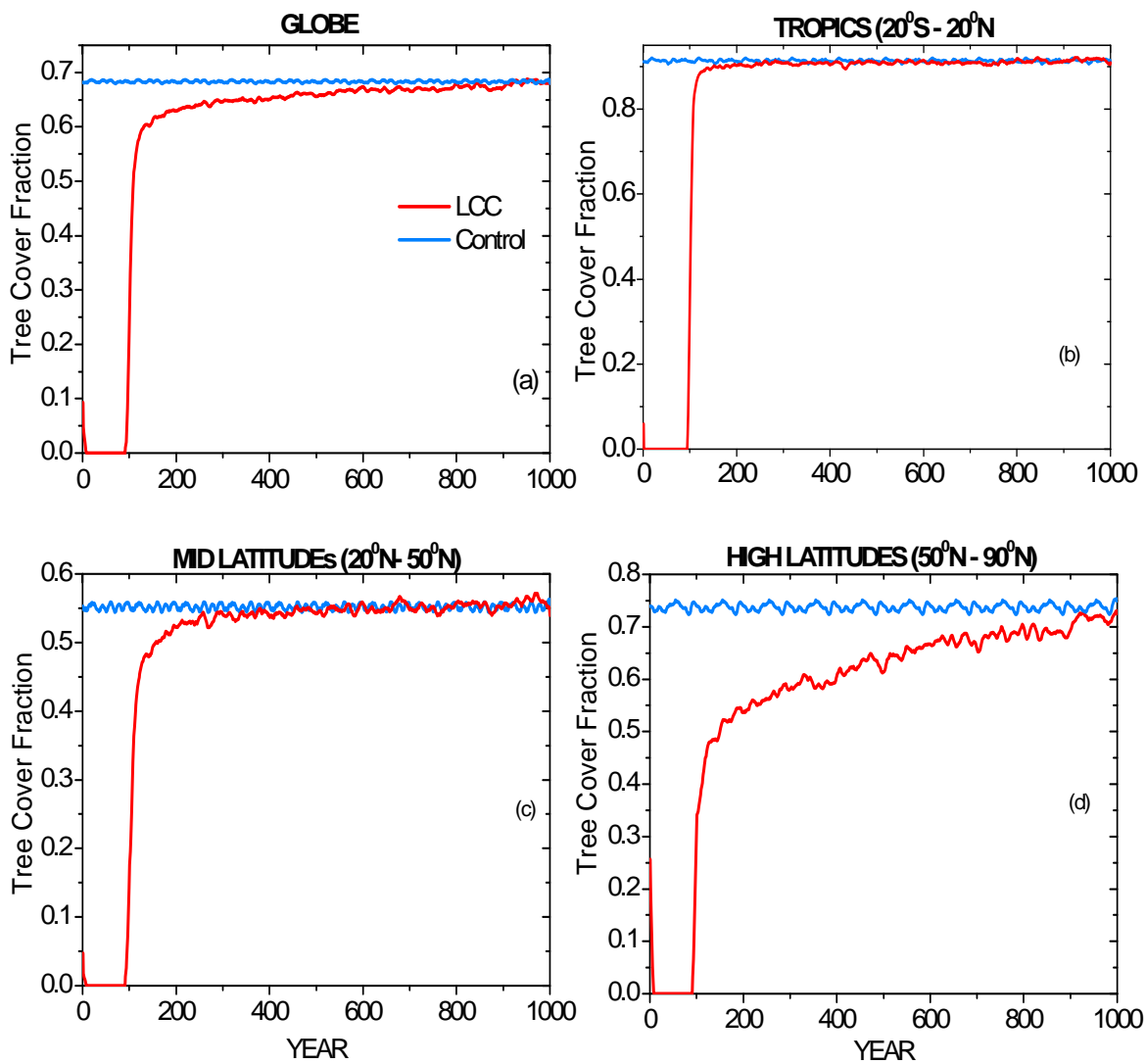
622

623



624
 625
 626
 627

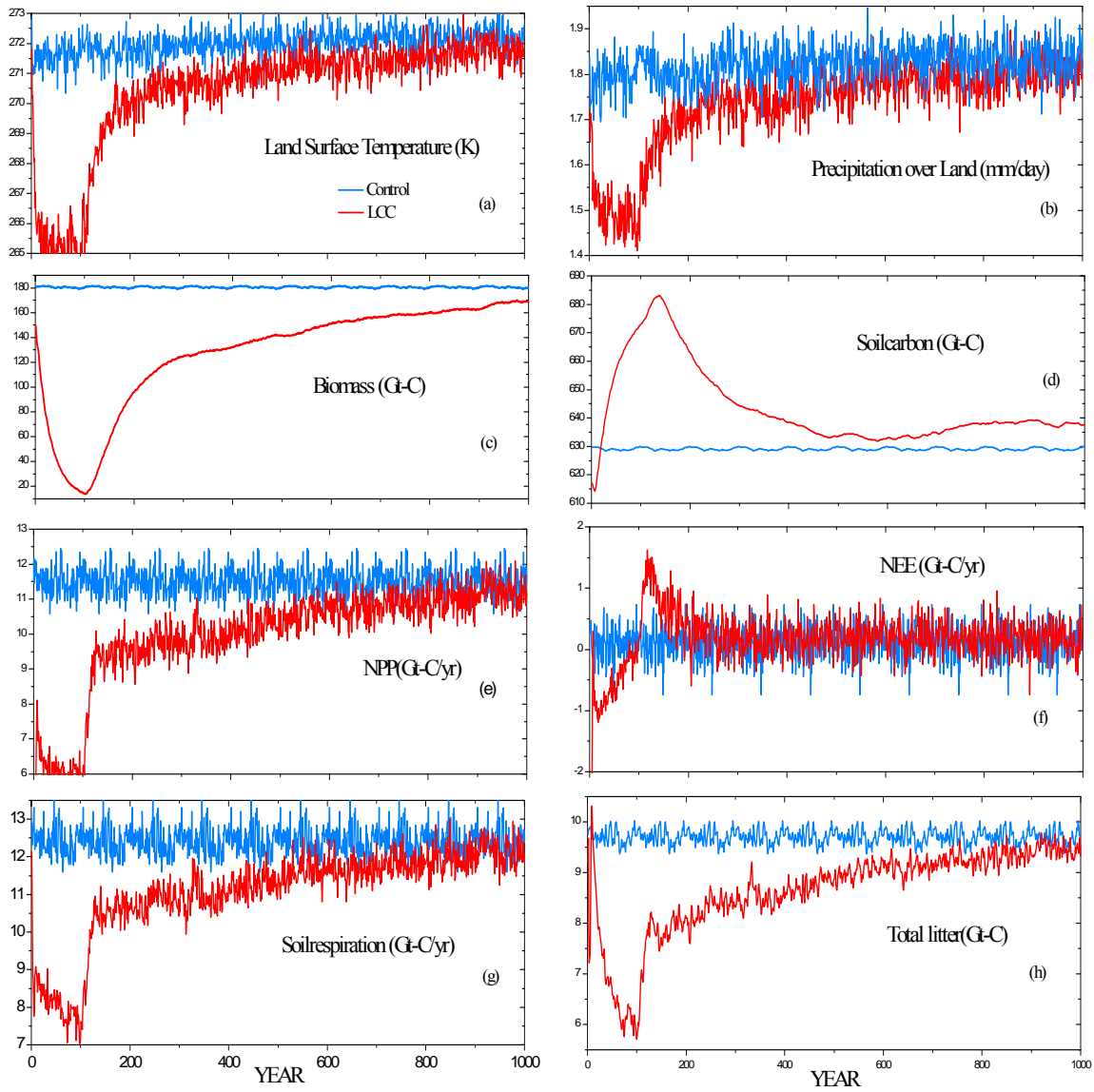
Figure 1



629
630
631
632

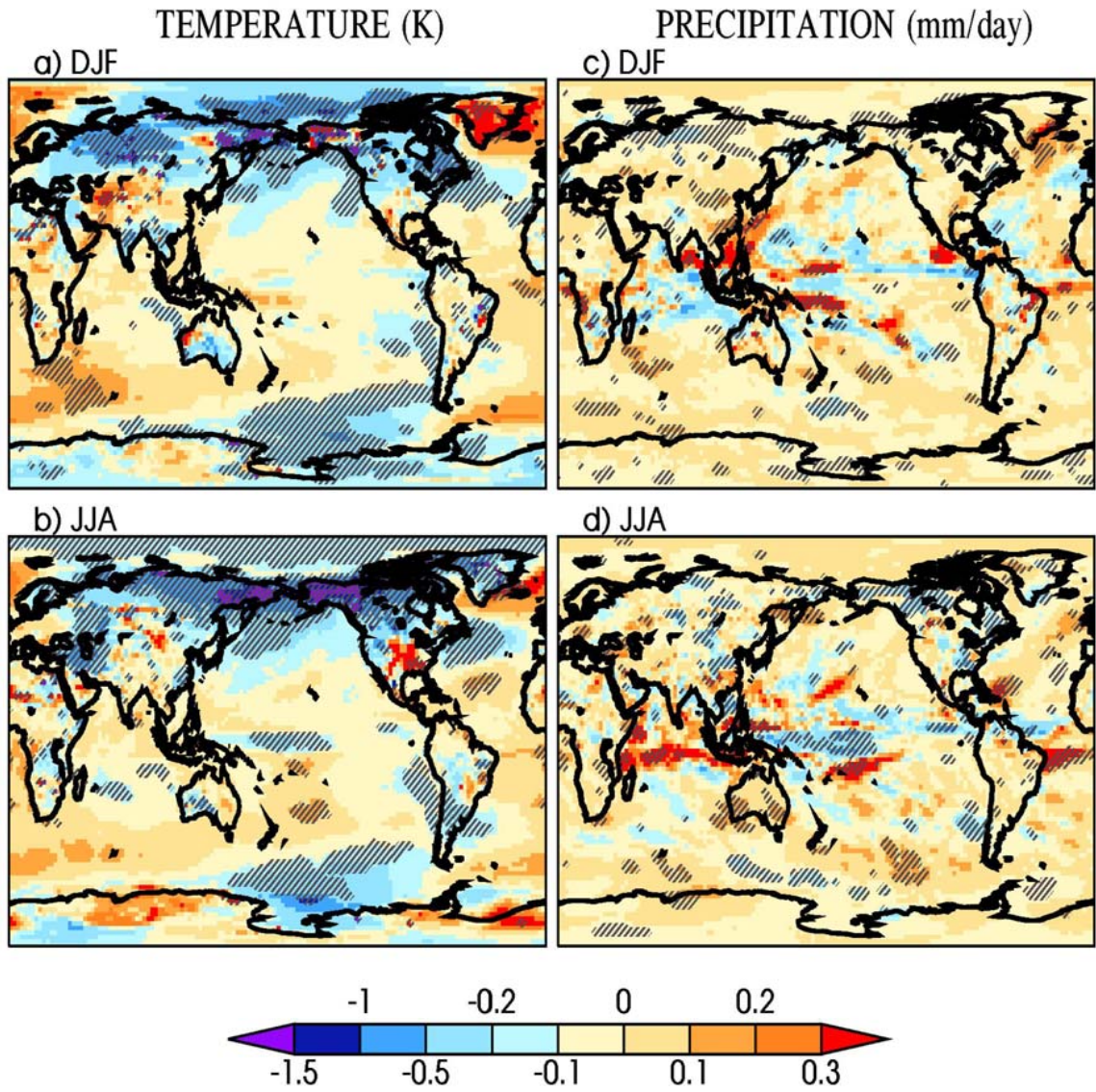
Figure 2

HIGH LATITUDES (50°N - 90°N)



633
634
635

Figure 3



636
 637
 638
 639

Figure 4

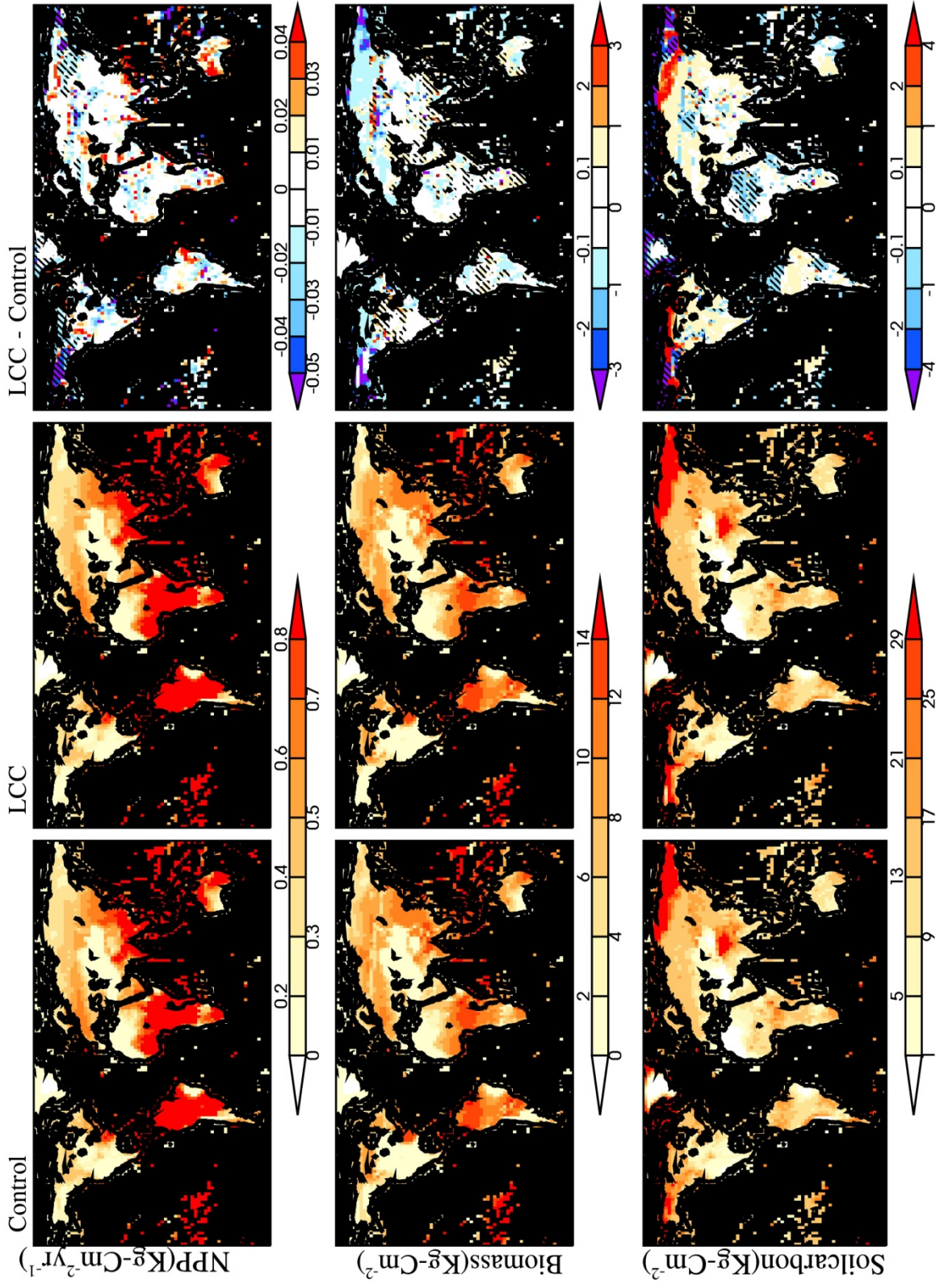


Figure 5

641
642
643